RESEARCH ARTICLE

Voltammetric and impedimetric analysis of adriamycin and fish sperm DNA interaction using pencil graphite electrodes

Pwadubashiyi Coston Pwavodi[1]

Abstract

The electrochemical behavior of fish sperm double-strand deoxyribonucleic acid (dsDNA) in the presence of adriamycin (ADR) is based on the reduction of the guanine?s oxidation peak signal and examined using electrochemical techniques with pencil graphite electrodes (PGEs). A hallmark for identifying Adriamycin was the reduction in the peak height of the guanine oxidation signal, following the interaction of the drug with dsDNA. Differential pulse voltammetry (DPV), electrochemical impedance spectroscopy (EIS), and cyclic voltammetry (CV) were the characterizing methods used in the investigation. The parameters employed for the optimization experiments to ascertain the electrochemical behavior of Adriamycin were Scan rate and pH investigations. The results of the characterization and optimization investigations demonstrated that the ADR immobilized at various concentrations on the electrode surface interacted with the 100 µg/mL dsDNA. According to the EIS findings, as dsDNA and ADR concentration increase, charge transfer resistance (Rct) decreases. When the electrochemical behavior of ADR was examined using different pH values and scan rates, peak currents at pH 4.0 were observed to be the strongest, with the peak values changing to the negative with the peak current signal increasing. Limits of detection (LOD) and quantitation (LOQ) were determined to be 0.0014 µM and 0.004 µM, respectively.

Graphical abstract
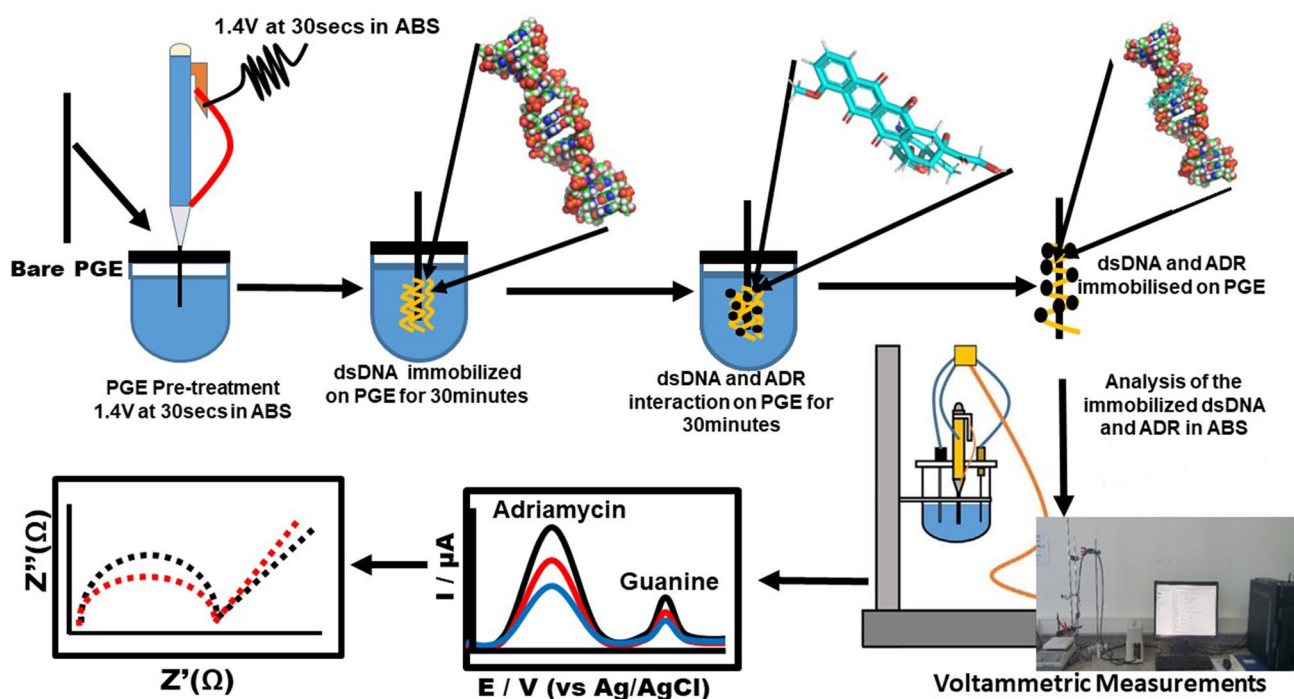
Extended author information available on the last page of the article

1 Introduction

To create a novel class of biosensors for detecting dsDNA interactions with other chemicals like contaminants or pharmaceuticals, nucleic acids have been electrochemically coupled with transducers. Given that these substances interact with the dsDNA, this detection aids in screening them as well [1]. Small molecules of drugs, chemicals, ligands, or other compounds can bind to DNA through covalent or non-covalent interactions. Covalent interactions between compounds and DNA can lead to irreversible chemical alterations of the DNA, leading to cell death. In contrast, non-covalent interactions between compounds and DNA occur with intermolecular forces weaker than covalent interactions and occasionally reversible [2?4]. Different electrochemical approaches have been used to look for interactions between DNA and anticancer drugs [5?8]. Other techniques, including molecular modeling, UV?Vis Spectroscopy, Fluorescence Spectroscopy, Nuclear Magnetic Resonance, Footprinting, Gel Electrophoresis, Mass Spectrometry, FTIR, Circular Dichroism Spectroscopy, Raman Spectroscopy, Capillary Electrophoresis, and Surface Plasmon Resonance (SPR), have been used for detection of DNA interaction with other compounds. These techniques have the benefits of being sensitive and selective. Still, they also have disadvantages. They require vast amounts of analytes for analysis, are difficult to use, take a long time, and require an extended period for sample pretreatment before analysis. Electrochemical methods have several advantages over more conventional ones, including inexpensive preparation costs, high sensitivity, equipment usability, selectivity, and a minimal requirement for analytes when comparing DNA and pharmacological molecules [2, 4?14].

The antibiotic adriamycin (ADR), a member of the anthracycline family (Fig. 1), has a wide range of uses in chemotherapy and has anti-neoplastic properties. The drug?s anticancer properties have been known for about 30 years [15, 16], but its mode of action in vivo has yet to be thoroughly characterized [17]. Understanding anticancer properties and their mechanisms of action are still crucial since doing so will help improve how it is administered. According to experimental data, ADR causes the DNA of malignant cells to have oxidative damage by producing reactive oxygen species [17?20]. It has been determined that the DNA?s guanine oxidation product is highly mutagenic and contributes to cell malfunction [21]. In 1972, X-ray crystallography and other techniques were used as proof to demonstrate that

ADR and other analogs in the family of anthracycline interact with the DNA intercalatively [15, 22?26]. The portion of the ADR that intercalates with the DNA base pairs when interacting with dsDNA is represented by the rings on its B and C sides (Fig. 1) [24, 25, 27, 28]. The DNA?s double helix minor groove still contains the ADR?s portion, which has amino sugar and its carbonyl side chain that binds to A. The DNA?s double helix main groove side is where the ring D extends [22, 27, 28]. The amino sugar has a positively charged amino group portion that interacts with the phosphate group of the DNA to perform its function and is crucial for intercalation and binding affinities to the dsDNA [23].

Graphite is advantageous as an electrode material because it combines the characteristics of metals and non-metals [29]. 4% graphite powder mixed with an inorganic resin, clay matrix, and cellulose is used to make pencils [30]. The Graphite-Reinforced Composite (GRC) is widely available commercially and is utilized as disposable material due to its high quality and low content of heavy metal impurities [31]. Graphite is a dark gray, soft, and porous material with adsorption capacity that is naturally abundant and highly conductive with an electrical conductivity for conducting polymer composites and electrical resistivity. The carbon atoms of the graphites are only bonded in two dimensions. It has a layered structure in which each carbon atom in graphite is sp2 hybridized. Three of each carbon atom?s four valence electrons form bonds with three other carbon atoms, while the fourth electron forms delocalized bonds that spread uniformly across all carbon atoms. The carbon atoms are hexagonally arranged in a planar condensed ring. The layers are stacked parallel to one another, with the atoms within the rings covalently bonded and the layers loosely bonded together by Van der Waal?s forces. Graphite?s anisotropic nature is caused by two types of bonding acting in opposite crystallographic directions. These two opposing chemical bonds may explain graphite?s ability to form a solid film lubricant. Because of the weak Van der Waal forces that govern the bonding between the individual layers, and because there are no bonds between the layers, the layers can easily slip off one another, making it an ideal lubricant and resulting in a lower coefficient of friction and, thus, wear. This is the same reason graphite is a good material for pencils ? layers come off and get left on the paper as you write. It conducts heat and electricity well along each layer of graphite but not perpendicular to it. The structure of graphite accounts for its high electrical conductivity. Graphite has

Fig. 1 Schematic representation of the intercalation activity of Adriamycin and dsDNA shown in the space-filing model. The Adriamycin is first depicted in 2D (top) and then in a 3D sticks model (down) with carbon atoms colored cyan inserted manually on the dsDNA. The dsDNA was retrieved from the Protein Data Bank (PDB) file 2MG8, and the Adriamycin was retrieved from the PubChem database (PubChem CID: 51,066,577)
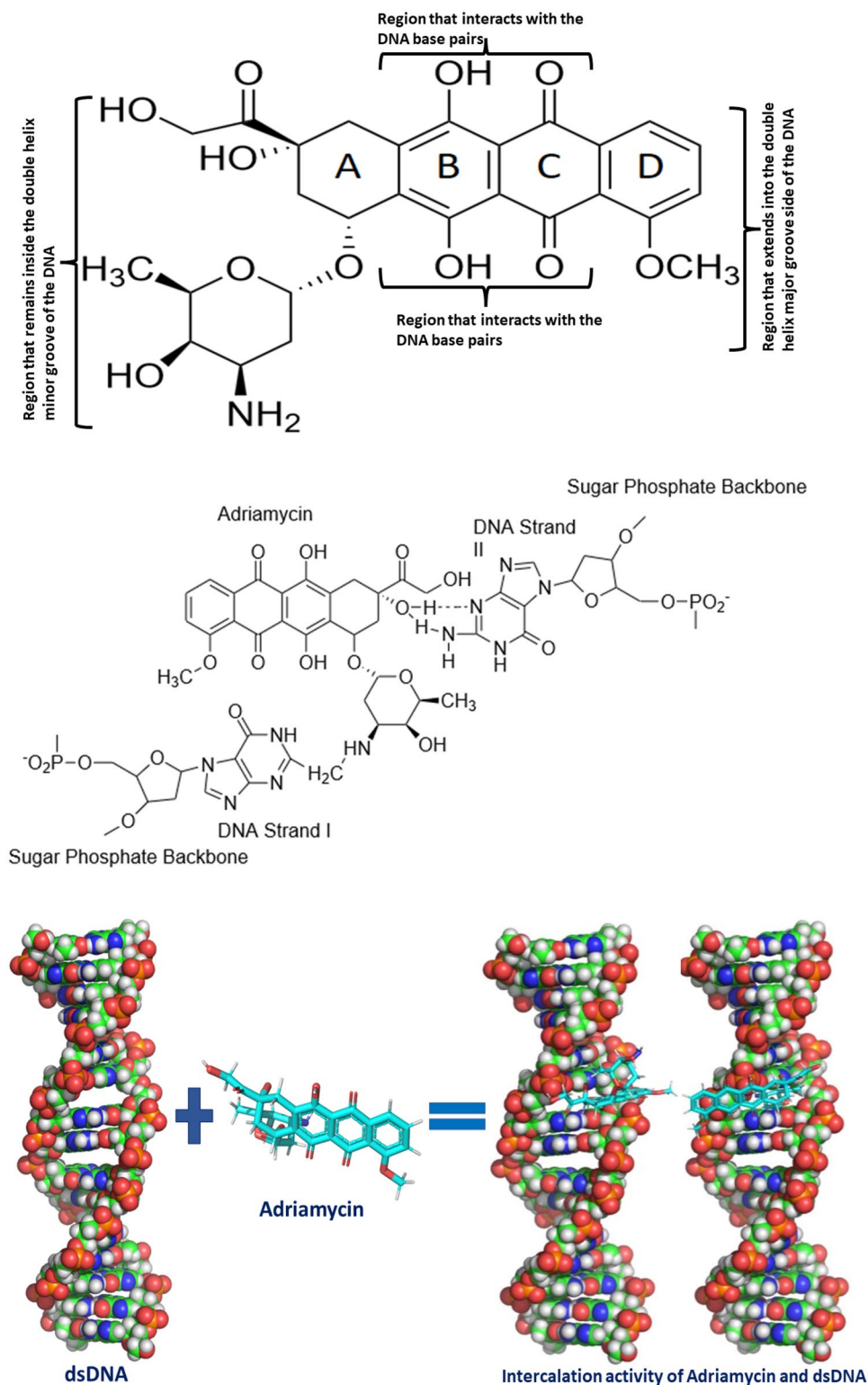
been used as electrode material in constructing disposable biosensors for detecting various analytes due to its good electro-catalytic properties [32?34]. With many studies and analyses of organic and inorganic chemicals reported by various academics worldwide in recent years, pencil graphite electrodes have grown in usefulness because of their electrochemical and economic properties. PGEs, which are easily disposable, are prepared from pencil graphite leads. They are easily accessible on the market, inexpensive, and user-friendly. PGEs show lower current signals than other

electrodes, their results are reproducible easily and highly sensitive, and their surface encourages adsorption. The electrode surfaces can be cleaned easily through pretreatment or application of a potential to activate the surface, thereby being used for different voltammetric techniques [35].

This study aims to use pencil graphite electrodes to detect fish sperm dsDNA and ADR interaction using voltammetric and impedimetric methods. To the best of our knowledge and after a thorough search, there are few reports on voltammetric and impedimetric techniques on dsDNA and ADR employing PGE (Table 1). Most of the works employed working electrodes such as carbon paste electrodes, glassy carbon electrodes, screen-printed electrodes, and other modified types of electrodes. Voltammetric methods like CV, DPV, and EIS are used in this study, and this work adds a report on the impedimetric analysis of dsDNA-ADR.

2 Experimental

2.1 Reagents

Fish sperm dsDNA was purchased from Sigma Aldrich in Istanbul, Turkey. 0.5 M of Acetate buffer solution (ABS) with a pH of 4.8 was combined with 20mM NaCl to create a stock solution of dsDNA at 1000 ppm (5 mg/5ml). Acetate buffer solutions (ABS) were prepared at a concentration of 0.5 M and various pH values ranging from 4.0 to 8.0. They were made according to conventional procedure using 0.5 M K_2HPO_4 milliliters (mL) and 0.5 M KH2PO4 milliliters (mL). The working solutions were created by diluting the

1.8 mM ADR stock solution with ultra-pure water to various concentrations (Fig. 2).

2.2 Apparatus

The AUTOLAB-PGSTAT204 and the program Nova 2.1.2 were used to perform voltammetric and impedimetric measurements. The analysis was performed using a three-electrode setup connected to the AUTOLAB. The three-electrode system includes the platinum wire-based auxiliary electrode, the Ag/AgCl/3MKCl reference electrode, and the PGEs working electrode.

### 2.3 Procedures for preparation, pretreatment, and immobilization

The Ultra-Polymer TOMBOW 0.5HB pencil leads were utilized for the analysis. They were purchased from Izmir at a stationery shop. They were divided into two halves with a length of 3.5 cm, and about 1.5 cm was marked with a white marker and used as the transducer (working electrode surface). The surface of the PGEs was cleaned in the pretreatment process by applying a potential at 1.4 volts (V) for 30 s using chronoamperometry to prevent contaminants and noise in the analysis. The procedure was repeated for each PGE.

2.4 dsDNA and ADR immobilizations on the pencil graphite electrodes? surface

Vial tubes containing 200 µL of fish sperm dsDNA were made as the working solution at a concentration of

Table 1 Comparison of recently published articles on Pencil Graphite Electrodes, drugs, and DNA

Compound	Method	Electrode	Medium	LOD	References
Daunorubicin	CV, DPV	PGE/CHIT-PGEs	pH 4.8 ABS and PBS 7.4	1.28 µM and 0.60 µM	[36]
Succinamic acid functionalized PAMAM dendrimer	DPV, CV, EIS	G2-PS/PGEs	pH 7.4 PBS	4.2 µg/mL	[37]
Idarubicin	DPV	dsDNA/PP/La_2O_3 NP@SF-L Cu_2S NS/PGE	pH 4.8 ABS	1.3 nM	[38]
Mitomycin C	DPV, CV,EIS	PoPD-MWCNT/PGE	pH 7.4 PBS and 4.8 ABS	0.012 mg $L^{?1}$	[39]
microRNA-34a	CV, EIS	IL/CA/PGEs	pH 7.4 PBS	109 nM	[40]
Dexrazoxane	CV, DPV	GRPox/PGE	pH 4.8 ABS	1.24 µg/mL	[41]
single-stranded DNA	CV	AuNPs/CB?PGE	pH 7.4 PBS	$1.0? \times ?10^{?9}$ M	[42]
l-lysine	CV	LOxNPs/GrONPs/PGE	pH 7.0 PBS	0.01 µM	[43]
Temodal	DPV,EIS,	dsDNA/AuNPs/PGE	pH 4.8 ABS	1.0 nM	[44]
daunorubicin	DPV	PGEs	pH 4.8 ABS	NS	[45]
DLD-1 cancer cells	EIS,CV	PNPs/PGE	pH 7.4 PBS	100 cells $mL^{?1}$	[46]
Dacarbazine	DPV,CV,EIS	SWCNT???PGE	pH 7.2 PBS	$1.10?µM$	[47]
Bleomycin	DPV,EIS	AuNPs/PGE	pH 4.8 ABS	NS	[48]
Doxorubicin	DPV,CV, EIS	dsDNA-MWNTs- Fe_2O_3/SnO_2-CHIT-PGE)	pH 7.0 PBS	0.004 nmol $L^{?1}$	[49]
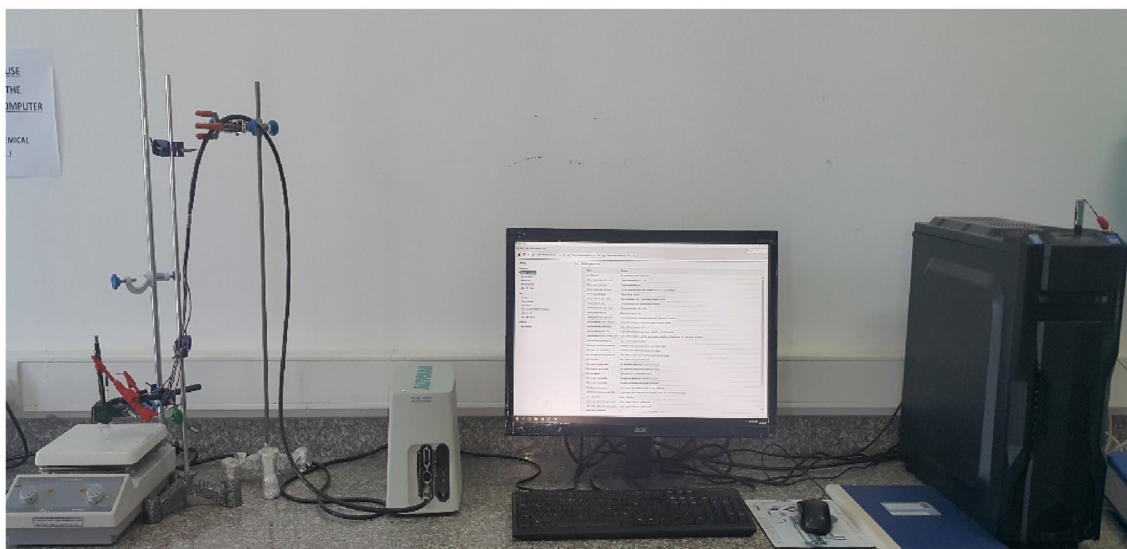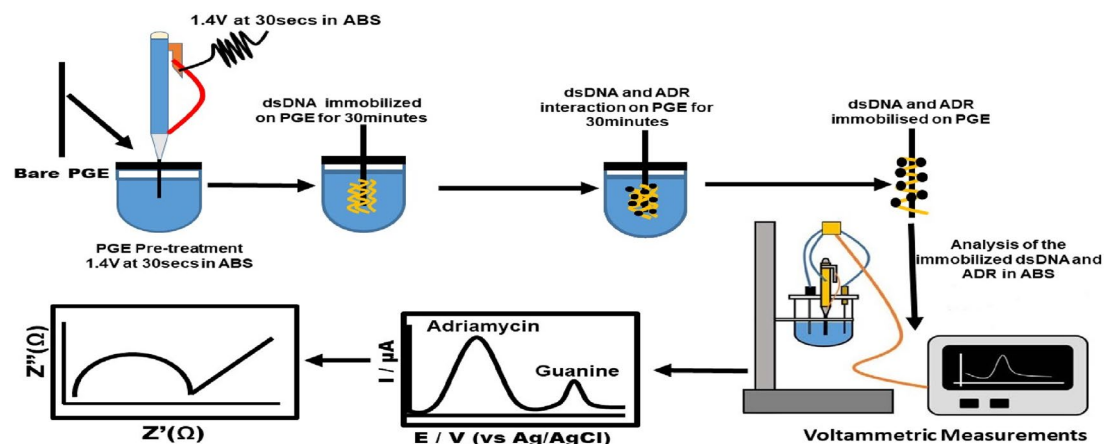
Fig. 2 Experimental Procedure of the electrochemical detection of the interaction between dsDNA and Adriamycin immobilized on Pencil Graphite Electrodes and the photo of the sensing setup

100 µg/mL, with the PGEs inserted into the vial tubes. All of the PGEs employed for the study had dsDNA immobilized on them for about 30 min. dsDNA was immobilized on the electrode surface of PGEs using an adsorption technique.

Different concentrations of solutions were prepared and used as working solutions from the stock solution of ADR. The PGEs inserted into the dsDNA solution were removed and inserted into vial tubes containing 74 µM of ADR. The immobilization was done for about 30 min. To get rid of unbound dsDNA and ADR, the PGEs were rinsed with ABS with a concentration of 0.5 M and a pH of 4.8 for 3 s.

For the pH study, the PGEs were immobilized in a 5 ml ADR working solution of 0.92 mM in a beaker for about 30 min, rinsed for 2 s in the ABS, and then used for the study (Fig. 2).

2.5 Electrochemical measurement technique

CV, DPV, and EIS measurements were employed for the study. A minimum of three rounds of experiments were made, with five PGEs being analyzed for each concentration. Their average values were then calculated and shown in the results section. Newly pre-treated PGEs were utilized in every round of repetition of the analysis to study the dsDNA and ADR interaction. The DPV measurements were performed in the acetate buffer solution. The scanning potential range employed for the measurements is +?0.15 V to +?1.4 V, and a scan rate of 10.071 mVs$^{?1}$ was used.

Then, the EIS measurements were performed using a redox solution of 2.5 mM [Fe (CN) 6]$^{3?/4?}$ produced in 0.1 M KCl. The measurement?s frequency range was between 100 kHz and 0.1 Hz. Using the AUTOLAB-PGSTAT204, the values for charge transfer resistance (Rct) were obtained

Fig. 3 Differential pulse voltammograms in pH 4.8, 0.5 M acetate buffer solution showing the signal of **A** 100 µg/mL, dsDNA only immobilized on bare PGE without interaction with ADR. **B** Adriamycin only with a concentration of 0.46 mM immobilized on bare PGE without interaction with dsDNA
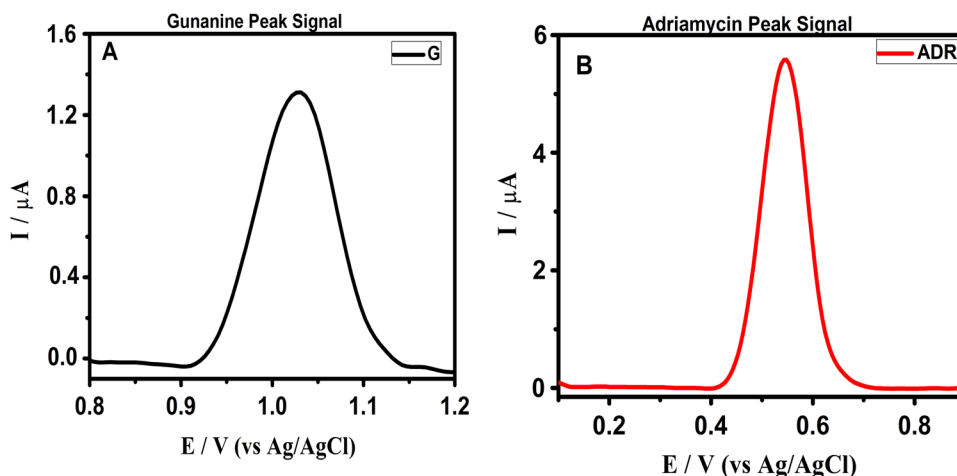
using the fit and simulation function in Nova 2.1.2 software, which corresponds with the semicircle diameter of the Nyquist plot.

Voltammetric techniques for CV and DPV were employed for the analysis in various buffer solutions prepared with a concentration of 0.5 M ABS at ranges from pH 4.0 to 8.0 for the pH analysis of the ADR. After each investigation, peak current signals for each measurement were recorded. The CV technique was employed with scan rates between 20, 40, 60, 80, 100, 200, 250, 300, 350, 400, and 450 mVs⁻¹, respectively (Figs. 2 and 6).

2.6 Preparation and detection of ADR in real samples

To employ the proposed fabricated biosensor in detecting ADR in real samples, urine samples were collected from a healthy individual and filtered. DPV was used to analyze the ADR in the spiked samples of urine. The voltammograms obtained were recorded using a standard addition method using serial dilutions of known concentrations and volumes of the ADR. A volume of 2 mL of urine was inserted into a beaker, and a known aliquot concentration of 0.03 mM and 0.05 mM of the ADR was added and made to a final volume of 10 mL using 0.5 M ABS at a pH of 4.8. They were then stirred up for 1 min using a magnetic stirrer. The measurements were recorded from the voltammograms of each beaker containing the urine and aliquots concentrations of ADR.

3 Results and discussion

3.1 Adriamycin and dsDNA electrochemical behavior on PGE

For the study on the interaction between dsDNA and ADR, the Differential Pulse Voltammetry technique was applied, and the guanine oxidation peak current signal of 100 µg/mL dsDNA was recorded at an oxidation potential of 1.0 to 1.1 V (Fig. 3A) [2, 50?52]. All of the results of the dsDNA and ADR interaction investigation repeatedly showed the guanine oxidation at this same potential. This is because guanine is suggested to be the most electroactive base of the dsDNA among other bases of the dsDNA. Thus, guanine is the marker for dsDNA interaction with other compounds. Using DPV measurements in ABS, the behavior of Adriamycin was only examined at 0.46 mM concentration (Fig. 3B). After applying a positive potential, the oxidation potential of ADR was found to be between 0.55 and 0.60 V[53].
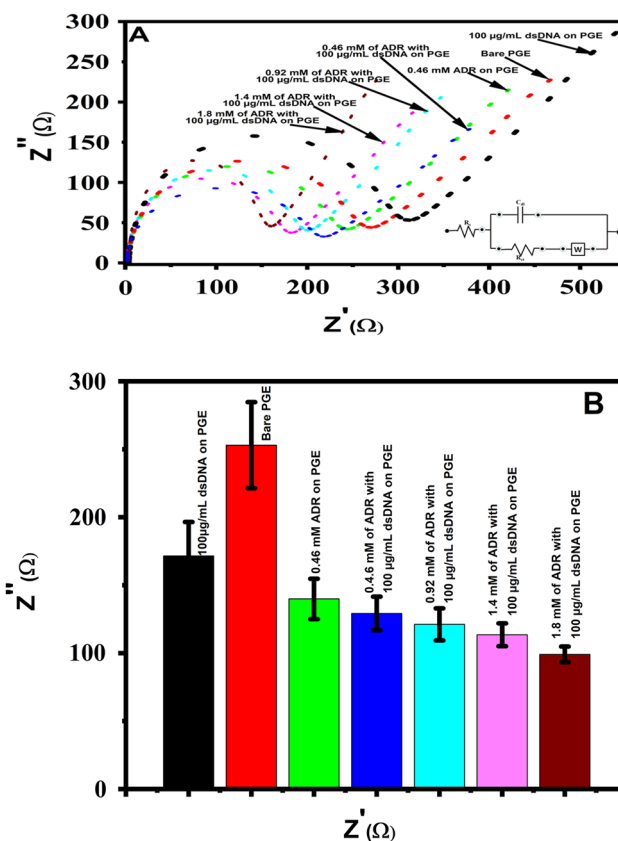
3.2 Electrochemical behavior of dsDNA and adriamycin interaction on PGE

DPV measurements were used to examine the electrochemical behavior of the interaction between dsDNA and ADR on PGEs (Fig. 4), showing the peak current signal response as ADR?s concentration increases with 100 µg/mL of dsDNA before and after the reaction. The increased concentration of ADR was from 0.46 mM, 0.92 mM, 1.4 mM, and 1.8 mM, respectively, as it interacts with the dsDNA. The peak current signal of the guanine signal is seen to be affected by the increase in ADR?s concentration, thereby gradually decreasing the guanine signal. Three assumptions can be suggested for this electrochemical behavior: (a) The ADR is attached to the dsDNA bases, shielding the oxidizable groups of the electroactive DNA bases; as a result, the peak current signal decreases with
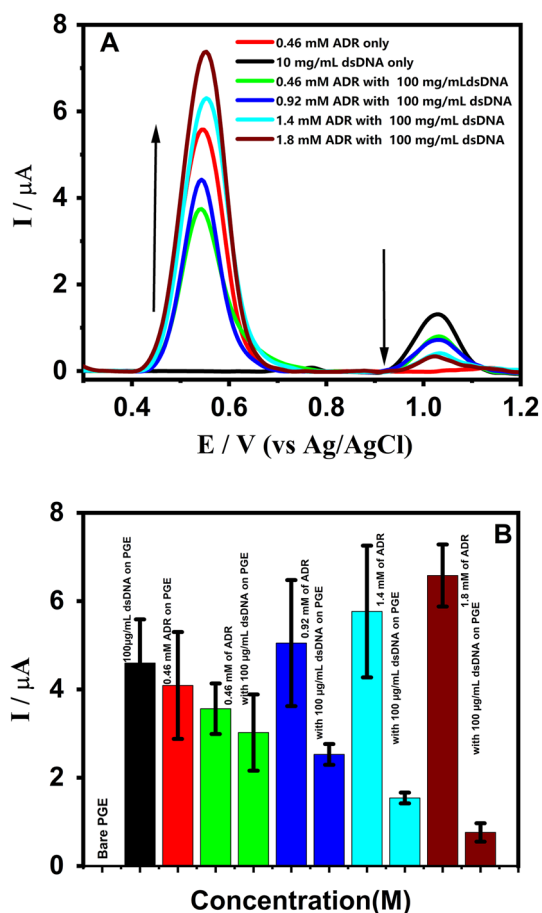
Fig. 4 A Differential pulse voltammograms and **B** bar plots show the different measurements in pH 4.8, 0.5 M ABS using PGEs. The labeled results on the voltammogram and the bar plots, respectively, represent Bare PGEs, 100 μg/mL of dsDNA only, 0.46 mM of ADR, 0.46 mM of ADR with 100 μg/mL dsDNA, 0.92 mM of ADR with 100 μg/mL dsDNA, 1.4 mM of ADR with 100 μg/mL dsDNA, 1.8 mM of ADR with 100 μg/mL dsDNA all immobilized on PGEs

Fig. 5 A showing the Nyquist diagrams for the R_{ct} values in the solution containing 5mM $K_3[Fe(CN)_6]/K_4[Fe(CN)_6]$ (1:1) with 0.5 M KCl by using Bare PGEs, 100 μg/mL dsDNA, 0.46 mM of ADR, 0.46 mM of ADR with 100 μg/mL dsDNA, 0.92 mM of ADR with 100 μg/mL dsDNA, 1.4 mM of ADR with 100 μg/mL dsDNA, 8?×?10^?3 M of ADR with 100 μg/mL dsDNA, all immobilized on PGEs **B** Bar charts showing the Rct values of the respective analysis performed on bare electrode PGE, dsDNA immobilized on PGE. DsDNA with ADR immobilized on the PGEs

increasing ADR concentration. This causes the drug to interact with dsDNA, especially at greater concentrations, and confine to the surface [52], (b) A marker of the ADR?s intercalation activity as a planar molecule into the dsDNA double helix structure is the decrease in the dsDNA guanine current peak signals [54]. The structure of ADR (Fig. 1) depicts the interaction between the drug and dsDNA by intercalation [55][56]. The aminosugar and carbonyl side chain of ADR connects to ring A to interact with the minor groove of the dsDNA. The B and C rings of ADR intercalate between the DNA bases. The positively charged aminosugar of the ADR binds to the phosphate backbone of the dsDNA as ring D extends to interact with the major groove of the dsDNA [22, 23, 27, 28]. (c) A decrease in the strength of the guanine signal oxidized at the PGEs surface could be suggested to be from modifications in the charge transfer characteristics of DNA due to its interaction with the medication [54, 57, 58].

3.3 Impedimetric investigation on the interaction between dsDNA and adriamycin on PGE showing their electrochemical behavior

The impedimetric analysis of the electrochemical behavior was conducted in the redox solution of 2.5 mM of [Fe (CN) 6]3-/4- prepared in 0.1 M KCl using a frequency of 100 kHz to 0.1Hz. The spectrum obtained (Fig. 5A) of the EIS measurement is for bare PGEs, 100 μg/mL dsDNA-modified PGEs, 0.46 mM ADR-modified PGEs, and ADR concentrations of 0.46 mM, 0.92 mM, 1.4 mM, and 1.8 mM with dsDNA, respectively, on PGEs. The charge transfer resistance (Rct) values related to the Randles-Sevcik circuit are evaluated in the inset (Fig. 5A). According to the results, the

Table 2 Linear regression equations for peak current Ip and the square root of scan rate, peak current Ip and scan rate, and the logarithm of anodic peak current and the logarithm of scan rate for ADR on PGEs

Adriamycin and PGEs	Regression Equation	R^2 Value
Ipa on $\nu^{1/2}$ (mVs^{-1})$^{1/2}$ (Controlled Diffusion)	Ipa(μA) = 211.98 $\nu^{1/2}$ (mVs^{-1})$^{1/2}$ − 18.77	0.9918
Ipa versus Scan Rate ν (mVs^{-1}) (Controlled Adsorption)	Ipa(μA) = 255.43 ν (mVs^{-1}) + 17.15	0.9930
log Ipa Versus log ν (mVs^{-1})	Log Ipa(μA) = 0.6623 log ν (mVs^{-1}) + 2.3270	0.9979

$\nu^{1/2}$ Square root of scan rate, *PGE* Pencil Graphite Electrode, (mVs^{-1})$^{1/2}$ = square root of volt per second. *Ipa* Anodic peak current

bare PGE «a» has an Rct value of 170 Ω, suggesting a slow electron transfer rate between the redox solution and electrode surface during the electrochemical reaction [59]. The Rct value for the dsDNA immobilized on the PGEs is 250 Ω (Fig. 5B), which is increased more than the bare PGE. This suggests successful adsorption of the dsDNA on the surface of the electrode and could also be attributed to the negatively charged dsDNA on the electrode surface and the electrostatic effect of the redox solution [60]. The Rct values of dsDNA and ADR decrease as concentration increases due to their immobilization on the electrode surface. The positive charges on the ADR balance the solution's negative charges, and this could indicate that the dsDNA and ADR interacted through intercalation activity [58, 60]. The Nyquist diagram contains the analysis's circuit model, which represents the corresponding impedance measurement, with Cdl as the charge capacitance, Rct as the charge transfer resistance,

and W as the Warburg impedance caused by mass transfer to the electrode surface, and Rs as the solution resistance [60].

3.4 Study of scan rate and its impact on adriamycin peak current

Cyclic voltammetry was used to show the effect of scan rate (Fig. 6A) on the electrochemical behavior of Adriamycin immobilized on the PGEs. The peak current signals of the ADR could be seen on the voltammogram to increase as the applied scan rates increased. From the observed results, a linear plot was done to obtain the equation of peak current Ip versus square root of scan rate $\nu^{1/2}$. This was done to indicate a typical diffusion-controlled reaction of the electrochemical behavior of ADR on the electrode surface (Fig. 6C; Table 2).

The peak currents Ip were plotted linearly against scan rate (ν), and a straight line was produced (Fig. 6B; Table 1). The results show a linear relationship where the scan rate
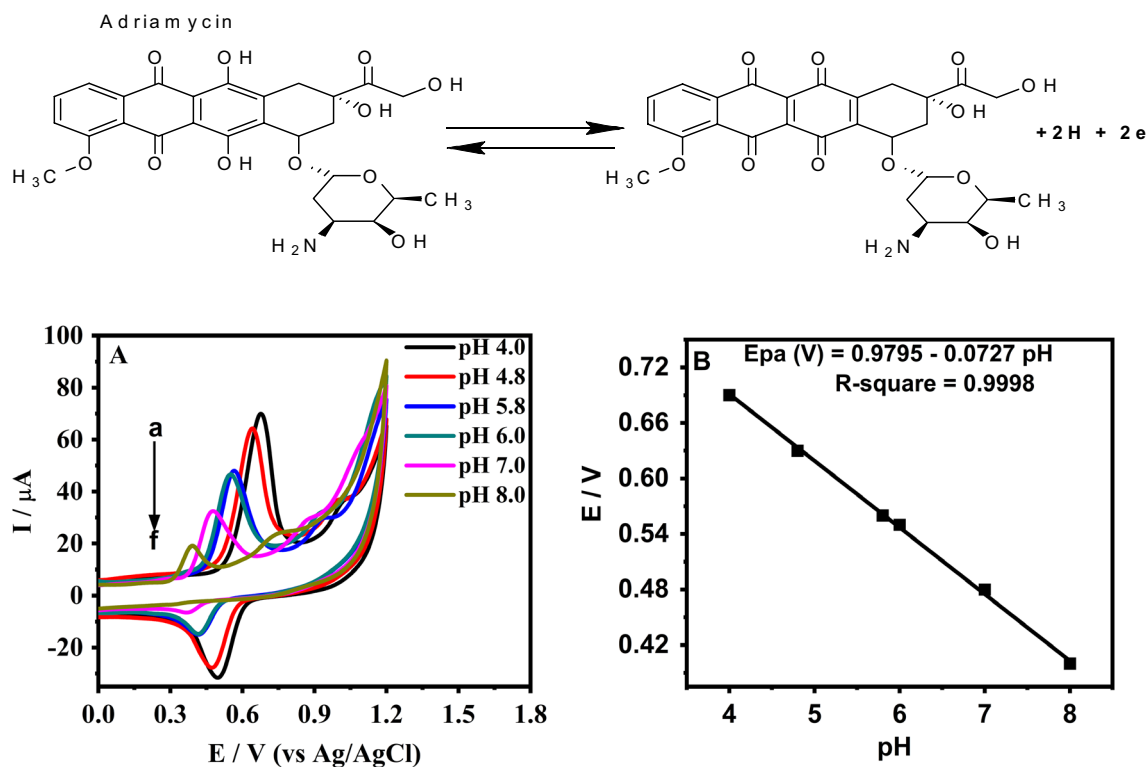
Fig. 6 **A** Cyclic voltammograms showing the electrochemical oxidation and reduction of ADR immobilized at PGEs in 0.5 M phosphate buffer of pH 4.0 at different applied scan rates of (20, 40, 60, 80, 100, 200, 250, 300, 350, 400, and 450) mVs^{-1}, respectively. **B** and **C** show the influence of peak current Ip on the square root of scan rate $\nu^{1/2}$ (mVs^{-1})$^{1/2}$ and scan rate ν (mVs^{-1}). **D** shows the logarithm of anodic peak current and the logarithm of scan rate (log Ip versus log ν (mVs^{-1}))
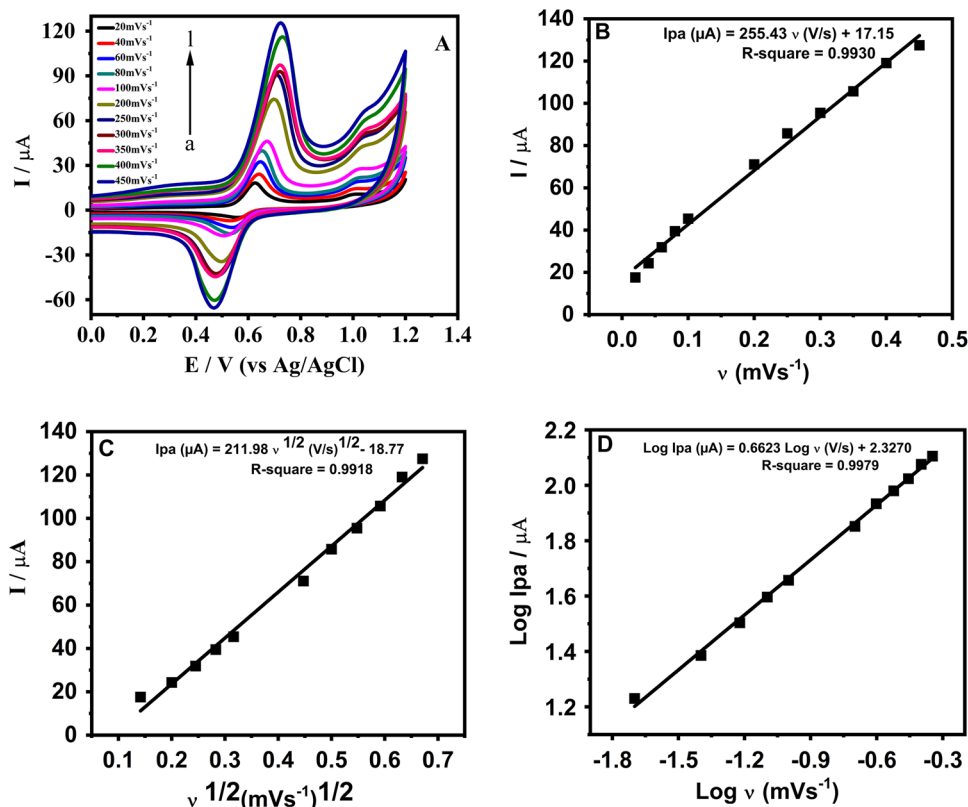
Table 3 The equation of anodic peak potentials (Epa) and pH with slope from cyclic voltammetry used in analyzing the pH of ADR at the PGE surface

Adriamycin (PGE)	Epa and the pH	Value of R^2	The slope of Epa/pH (mV/pH)	Nernstian number (mV/pH)
Regression Equation of Anodic Peak Potentials	Epa (V)?=?0.9795?0.0727 pH	0.9998	72	59

Fig. 7 A Cyclic voltammograms showing the effect of pH on the electrochemical behavior of the ADR on PGE in 0.5 M PBS with pH of 4.0, 4.8, 5.8, 6.0, 7.0, and 8.0 at a scan rate of 200 mVs⁻¹, respectively. **B** shows a Linear regression plot, anodic peak potentials (Epa) equation, and the pH of ADR for cyclic voltammetry used in analyzing the electrochemical behavior of ADR at the PGE surface

Fig. 8 The calibration curve and histogram of the different concentrations of the ADR in the range of 9.19 µM, 7.36 µM, 5.5 µM, 3.67 µM, and 1.84 µM immobilized on the PGEs in 0.5 M PBS pH 4.0 used for obtaining the LOD and LOQ in the main work
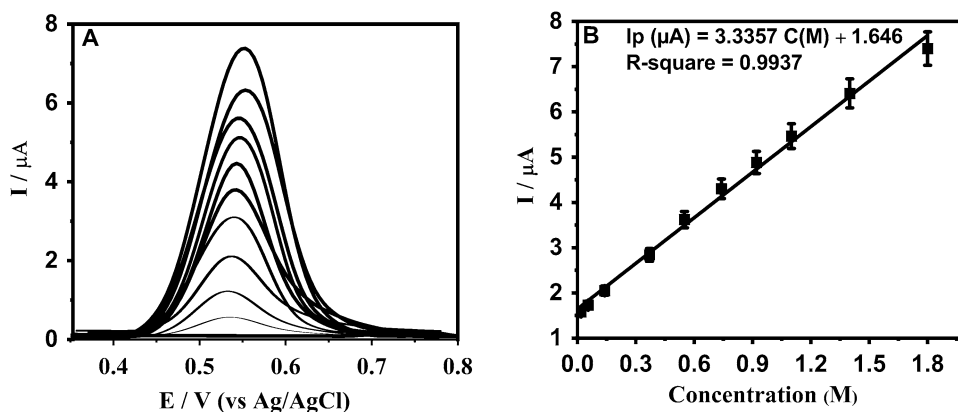
Table 4 The LOD and LOQ of ADR compared to other methods used to determine ADR.

Electrode	Modifier	Method	Linear range (μM)	LOD (μM)	References
GCE	MWCNTs/AgNPs	CV, DPV	0.0008?0.019	0.002	[61]
GCE	PS/Fe$_3$O$_4$-GO- SO$_3$H	DPV	0.043-3.5	0.0049	[62]
CPE	Carbon paste	DPV	0.1?10	0.01	[63]
CPE	No modifier	CV, DPV	0.01?100	?	[64]
GCE	DNA sensor	DPV, Impedimetric	0.001-100	0.0001	[65]
GCE	GQD	CV, DPV	0.02?3.6	0.016	[66]
Pt	MWCNTs	CV	0.09?7.36	0.003	[67]
PGE	No modifier	CV, DPV, EIS	0.018?1.8	0.0014	This study

GCE Glassy Carbon Electrode, *MWCNTs/AgNPs* Multi-walled carbon nanotubes/Silver nanoparticles, *CPE*?Carbon paste electrode, Electropolymerized Neutral Red/polycarboxylated thiacax [4] aren/DNA, *GQD* Graphene quantum dots, *Pt* Platinum, *CV* cyclic voltammetry, *DPV* differential voltammetry
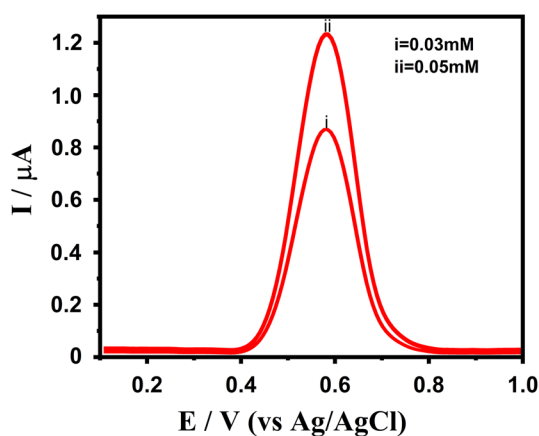
Fig. 9 DPV was obtained using PGE in a mixture of 0.03 mM and 0.05 mM ADR in urine samples and 0.5 M ABS pH 4.8

increases with anodic and cathodic peak currents, suggesting that the oxidation reaction is quasi-reversible. To determine whether the electrochemical reaction that occurred on the electrode surface whether it is diffusion or adsorption controlled, the logarithm of scan rate and anodic peak current (log v (mVs$^{?1}$) versus log Ipa) technique was used (Fig. 6D; Table 2). The analysis showed that the slope was almost 0.5, indicating that the electrochemical processes that took place in the ADR analysis were diffusion controlled [59].

3.5 The effect of a pH study on the oxidation of adriamycin at PGEs

Cyclic voltammetry was applied, and the current response of ADR oxidation at PGE was investigated to identify its electrochemical behavior as a function of the buffer solution?s pH effect (Fig. 7A). The different pH values of the buffer solutions impacted the oxidation activity of the ADR on the surface of PGE, which changed its electrochemical behavior.

The ADR?s anodic peak currents (Ipa) and potentials (Epa) indicated a gradual decrease as the pH values increased from 4.0 to 8.0. The cyclic voltammograms of the electrochemical behavior of ADR suggested that the electrochemical alterations to the behavior of ADR at the electrode surface are distinctly pH dependent, causing the anodic peak current to decrease when the pH values are increased. This result causes the peak potentials to shift negatively to the left, demonstrating a linear regression relationship between the pH values and the anodic peak potentials (Epa) (Fig. 7B; Table 3). The Nernstian value of 59 mV/pH is the value for two electrons and two protons involved in oxidation and reduction reaction processes, and 29.5 mV/pH for processes involving two electrons and one proton reaction, the value derived from the result of the slope of Epa and pH relationship when compared to the Nernstian value, indicates that the reaction is a two-electron/two-proton oxidation and reduction reaction process [59].

3.6 Adriamycin?s LOD and LOQ

Differential pulse voltammetry was applied, and the effect of increasing the concentration of ADR was investigated at PGE using oxidation signals (Fig. 8). Based on the findings of the voltammetric method used, the limit of detection (LOD), and limit of quantification (LOQ) were determined. The ADR was studied from 0.018 μM to 1.8 μM in concentration. The LOD and LOQ for ADR were calculated using the peak currents using Eqs. (1) and (2), respectively.

$$LOD = 3 * Sa/b, \tag{1}$$

$$LOQ = 10 * Sa/b. \tag{2}$$

The variables ?Sa? and ?b? stand for our calibration curve?s slope and standard deviation, respectively. The detected ADR oxidation signals increased as the drug?s concentration gradually increased. Voltammogram studies

Table 5 Determination of ADR in the real sample of urine

Sample	Added(mM)	Found(mM)	Recovery (%)	Relative error
Urine	0	Undetected	?	?
	0.03	0.0305	101.67	±?1.67
	0.05	0.0494	98.8	±?1.2

revealed a linear association between peak currents signals and increased ADR concentration. The resulting equation, $Ip?=?3.3357\ C?+?1.646$ (Ip: µA, C: mol $L^{?1}$, and $R2?=?0.9937$), shows a linear regression. The LOD and LOQ results reported by other authors were compared with the computed detection limits of the drug ADR (Table 4).

3.7 Application of the fabricated biosensor in real samples

The detection of the presence of ADR in urine samples was carried out using PGE. The detection was first done with diluted 10 mL urine samples, which were blanks. DPV of the urine samples was analyzed without the presence of the ADR. The biosensor detected that the urine samples did not contain the presence of ADR. Aliquots of known concentration of ADR added to the urine samples were observed using DPV (Table 5). The oxidation peaks of the spiked ADR in the urine samples increased as the concentration of the ADR was increased (Fig. 9). The PGE detected the presence of the added standard ADR in the urine samples, with recoveries at almost 100%.

4 Conclusions

The results from voltammetric techniques demonstrated that the interaction between dsDNA and ADR on the surface of PGE resulted in a reduction in the guanine signals. ADR is pH dependent, as shown by the electrochemical behavior of ADR adsorbed on the PGEs under various pH values. According to the EIS study, PGE showed decreasing charge transfer resistance when our dsDNA and ADR concentrations increased between the electrode surface and the redox solution. As there is little to no research on the electrochemical impedance spectroscopy (EIS) of dsDNA and ADR using PGE, this voltammetric and impedimetric study also adds a report on the interaction of dsDNA and ADR that is employing pencil graphite electrodes. The DNA biosensor proved easy to make, affordable, and time-efficient. The LOD and LOQ results were compared to other biosensors reported in different literature and were close to or less than the reported biosensors. The proposed sensor was applied in real sample of urine to determine ADR in the sample of urine with 100% recoveries.

Declarations

Conflict of interest There are no conflicts to declare.

References

1. McGown LB, Joseph MJ, Pitner JB et al (1995) The nucleic acid ligand. A new tool for molecular recognition. Anal Chem 67:663A?8A. https://doi.org/10.1021/ac00117a002
2. Topkaya SN, Cetin AE (2019) Determination of electrochemical interaction between 2-(1H-benzimidazol-2-yl) phenol and DNA sequences. Electroanalysis 31:1571?1578. https://doi.org/10.1002/elan.201900199
3. Chu X, Shen G, Jiang J, Yu R (1999) Intercalation of pharmorubicin anticancer drug to DNA studied by cyclic voltammetry with analytical applications. Anal Lett 32:717?727
4. Topkaya SN, Karasakal A, Cetin AE et al (2020) Electrochemical characteristics of a novel pyridinium salt as a candidate drug molecule and its Interaction with DNA. Electroanalysis 32:1780?1787. https://doi.org/10.1002/elan.202000012
5. Kurucsev T, Kubista M (1992) Linear dichroism spectroscopy of nucleic acids. Q Rev Biophys 25:51?170. https://doi.org/10.1017/S0033583500004728
6. Lown JW, Hanstock CC, Bradley BD, Scraba DG (1984) Interactions of the antitumor agents mitoxantrone and bisantrene with deoxyribonucleic acids studied by electron microscopy. Mol Pharmacol 25:178?184
7. Fritzsche H, Akhebat A, Taillandier E et al (1993) Structure and drug interaction of parellel-stranded DNA studies by infrared spectroscope and fluorence. Nucleic Acids Res 21:5085?5091. https://doi.org/10.1093/nar/21.22.5085
8. Nunn CM, Van Meervelt L, Zhang S et al (1991) DNA-drug interactions. The crystal structures of d(TGTACA) and d(TGATCA) complexed with daunomycin. J Mol Biol 222:167?177. https://doi.org/10.1016/0022-2836(91)90203-I
9. Erdem A, Meric B, Kerman K et al (1999) Detection of interaction between metal complex indicator and DNA by using electrochemical biosensor. Electroanal An Int J Devoted to Fundam Pract Asp Electroanal 11:1372?1376.
10. Purushothama HT, Nayaka YA, Vinay MM et al (2018) Pencil graphite electrode as an electrochemical sensor for the voltammetric determination of chlorpromazine. J Sci Adv Mater Devices 3:161?166. https://doi.org/10.1016/j.jsamd.2018.03.007
11. Plambeck JA, William Lown J (1984) Electrochemical studies of antitumor antibiotics V. An electrochemical method of measurement of the binding of doxorubicin and daunorubicin derivatives to DNA. J Electrochem Soc 131:2556. https://doi.org/10.1149/1.2115358
12. Fojta M, Doffková R, Paleček E (1996) Determination of traces of RNA in submicrogram amounts of single- or double-stranded DNAs by means of nucleic acid-modified electrodes. Electroanalysis 8:420?426. https://doi.org/10.1002/elan.1140080504
13. Teijeiro C, Perez P, Marín D, Paleček E (1995) Cyclic voltammetry of mitomycin C and DNA. Bioelectrochem Bioenerg 38:77?83. https://doi.org/10.1016/0302-4598(95)01791-C
14. Erdem A, Kerman K, Meric B et al (1999) DNA electrochemical biosensor for the detection of short DNA sequences related to the

hepatitis B Virus. Electroanal Int J devoted Fundam Pract Asp Electroanal 11:586?587.

15. Perry CM (1996) The Chemotherapy Source Book. William & Wilkins. Awaverly Company, USA p3-4, pp.19-20.

16. Di AM, Gaetani M, Scarpinato B (1969) Adriamycin (NSC-123,127): a new antibiotic with antitumor activity. Cancer Chemother reports 53:33?37

17. Kiyomiya KI, Matsuo S, Kurebe M (2001) Differences in intracellular sites of action of adriamycin in neoplastic and normal differentiated cells. Cancer Chemother Pharmacol 47:51?56. https://doi.org/10.1007/s002800000201

18. Zhou S, Starkov A, Froberg MK et al (2001) Cumulative and irreversible cardiac mitochondrial dysfunction induced by doxorubicin. Cancer Res 61:771?777

19. Minotti G (1999) Erratum: role of iron in anthracycline cardiotoxicity: new tunes for an old song? (FASEB Journal (199?212)). FASEB J 13:594. https://doi.org/10.1096/fasebj.13.3.594

20. Kostoryz EL, Yourtee DM (2001) Oxidative mutagenesis of doxorubicin-Fe(III) complex. Mutat Res - Genet Toxicol Environ Mutagen 490:131?139. https://doi.org/10.1016/S1383-5718(00)00158-3

21. David SS, Williams SD (1998) Chemistry of glycosylases and endonucleases involved in base-excision repair. Chem Rev 98:1221?1261. https://doi.org/10.1021/cr980321h

22. Pigram WJ, Fuller W and LDH (1972) Stereochemistry of intercalation: interaction of daunomycin with DNA. Nat New Biol 235:17?19

23. Berg H, Horn G, Luthardt U, Ihn W (1981) Interaction of anthracycline antibiotics with biopolymers: part V. Polarographic behavior and complexes with DNA. Bioelectrochem Bioenerg 8:537?553. https://doi.org/10.1016/S0022-0728(81)80246-X

24. Frederick CA, Williams LD, Ughetto G et al (1990) Structural comparison of anticancer drug-DNA complexes: adriamycin and daunomycin. Biochemistry 29:2538?2549. https://doi.org/10.1021/bi00462a016

25. Lipscomb LA, Peek ME, Zhou FX et al (1994) Water Ring structure at DNA interfaces: Hydration and Dynamics of DNA-Anthracycline complexes. Biochemistry 33:3649?3659. https://doi.org/10.1021/bi00178a023

26. Zunino F, Gambetta R, Di Marco A et al (1977) The interaction of adriamycin and its beta anomer with DNA. Biochim Biophys Acta 476:38?46

27. Cullinane C, Phillips DR (1990) Induction of stable transcriptional blockage sites by adriamycin: GpC specificity of apparent adriamycin-DNA adducts and dependence on Iron(III) ions. Biochemistry 29:5638?5646. https://doi.org/10.1021/bi00475a032

28. Wang J, Ozsoz M, Cai X et al (1998) Interactions of antitumor drug daunomycin with DNA in solution and at the surface. Bioelectrochem Bioenerg. https://doi.org/10.1016/S0302-4598(98)00075-0

29. Chehreh Chelgani S, Rudolph M, Kratzsch R et al (2016) A review of graphite beneficiation techniques. Min Process Extr Metall Rev 37:58?68. https://doi.org/10.1080/08827508.2015.1115992

30. Alipour E, Majidi MR, Saadatirad A et al (2013) Simultaneous determination of dopamine and uric acid in biological samples on the pretreated pencil graphite electrode. Electrochim Acta 91:36?42. https://doi.org/10.1016/j.electacta.2012.12.079

31. Aoki K, Okamoto T, Kaneko H et al (1989) Applicability of graphite reinforcement carbon used as the lead of a mechanical pencil to voltammetric electrodes. J Electroanal Chem 263:323?331. https://doi.org/10.1016/0022-0728(89)85102-2

32. Mirceski V, Gulaboski R, Lovric M et al (2013) Square-wave voltammetry: a review on the recent progress. Electroanalysis 25:2411?2422

33. Alhadeff Eand Bojorge N (2011) ?Graphite-composites alternatives for electrochemical biosensor.? In metal, ceramic and polymeric composites for various uses. Intech Open, London

34. Tanzi MC, Farè S, Candiani G (2019) Chapter 1-Organization, structure, and properties of materials. Foundations of biomaterials engineering 10

35. David IG, Popa DE, Buleandra M (2017) Pencil graphite electrodes: a versatile tool in electroanalysis. J Anal Methods Chem. https://doi.org/10.1155/2017/1905968

36. Congur G, Eksin E, Erdem A (2019) Sensing and bio-sensing research chitosan modified graphite electrodes developed for electrochemical monitoring of interaction between daunorubicin and DNA. Sens Bio-Sens Res 22:100255. https://doi.org/10.1016/j.sbsr.2018.100255

37. Congur G, Eksin E, Mese F, Erdem A (2014) Sensors and actuators B: chemical succinamic acid functionalized PAMAM dendrimer modified pencil graphite electrodes for voltammetric and impedimetric DNA analysis. Sens Actuators B Chem 201:59?64. https://doi.org/10.1016/j.snb.2014.03.104

38. Mehdi M, Jahani S (2022) Investigation of a high-sensitive electrochemical DNA biosensor for determination of Idarubicin and studies of DNA-binding properties. Microchem J 179:107546. https://doi.org/10.1016/j.microc.2022.107546

39. Kuralay F, Bayramlı Y (2021) Electrochemical determination of Mitomycin C and its Interaction with double-stranded DNA using a poly (o -phenylenediamine) -Multi-Walled Carbon Nanotube Modified Pencil Graphite Electrode Electrochemical determination of Mitomycin C and. Anal Lett 54:1295?1308. https://doi.org/10.1080/00032719.2020.1801710

40. Kesici E, Eksin E, Erdem A (2018) An impedimetric biosensor based on ionic liquid-modified graphite electrodes developed for microRNA-34a detection. Sens (Switzerland). https://doi.org/10.3390/s18092868

41. Akpınar F, Şensoy KG, Muti M (2023) Electrochemical determination of dexrazoxane by Differential Pulse Voltammetry (DPV) using a Graphene Oxide Nanosheet Modified Pencil Graphite Electrode (PGE) Electrochemical determination of dexrazoxane by Differential Pulse Voltammetry (DPV) using a Graphene. Anal Lett 56:630?642. https://doi.org/10.1080/00032719.2022.2095567

42. Moustakim H, Mohammadi H, Amine A (2022) Electrochemical DNA Biosensor Based on Immobilization of a Non-Modified ssDNA Using Phosphoramidate-Bonding Strategy and Pencil Graphite Electrode Modified with AuNPs/CB and Self-Assembled Cysteamine Monolayer. Sensors 22(23):9420

43. Nohwal B, Chaudhary R, Pundir CS (2020) Amperometric L -lysine determination biosensor ampli fi ed with L -lysine oxidase nanoparticles and graphene oxide nanoparticles. Process Biochem 97:57?63. https://doi.org/10.1016/j.procbio.2020.06.011

44. Jahandari S, Ali M, Karimi-maleh H, Khodadadi A (2019) A powerful DNA-based voltammetric biosensor modified with au nanoparticles, for the determination of Temodal ; an electrochemical and docking investigation. J Electroanal Chem 840:313?318. https://doi.org/10.1016/j.jelechem.2019.03.049

45. Muti M, Muti M (2018) Electrochemical monitoring of the interaction between anticancer drug and DNA in the presence of antioxidant. Talanta 178:1033?1039. https://doi.org/10.1016/j.talanta.2017.08.089

46. Tugce Y, Akbal Ö, Bolat G et al (2018) Biosensors and bioelectronics peptide nanoparticles (PNPs) modi fi ed disposable platform for sensitive electrochemical cytosensing of DLD-1 cancer cells. Biosens Bioelectron 104:50?57. https://doi.org/10.1016/j.bios.2017.12.039

47. Kanat E, Eksin E, Karacicek B, Erac Y (2018) Electrochemical detection of interaction between dacarbazine and nucleic acids in

comparison to agarose gel electrophoresis. Anal Biochem. https://doi.org/10.1002/elan.201800064

48. Heydari-bafrooei E, Amini M, Saeednia S (2017) Electrochemical detection of DNA damage induced by bleomycin in the presence of metal ions. J Electroanal Chem 803:104?110. https://doi.org/10.1016/j.jelechem.2017.09.031

49. Taei M, Salavati H, Hasanpour F, Shafiei A (2015) Biosensor based on ds-DNA-decorated Fe 2 O 3/SnO 2-chitosan modified multiwalled carbon nanotubes for biodetection of doxorubicin. IEEE Sensors Journal 16(1):24–31

50. Zhao J, Hu GZ, Yang ZS, Zhou YY (2007) Determination of 1-naphthol with denatured DNA-modified pretreated glassy carbon electrode. Anal Lett 40:459?470. https://doi.org/10.1080/00032710600964759

51. Topkaya SN, Ozyurt VH, Cetin AE, Otles S (2018) Nitration of tyrosine and its effect on DNA hybridization. Biosens Bioelectron 102:464?469. https://doi.org/10.1016/j.bios.2017.11.061

52. Erdem A, Muti M, Papakonstantinou P et al (2012) Graphene oxide integrated sensor for electrochemical monitoring of mitomycin C-DNA interaction. Analyst 137:2129?2135. https://doi.org/10.1039/c2an16011k

53. Oliveira-Brett AM, Vivan M, Fernandes IR, Piedade JAP (2002) Electrochemical detection of in situ adriamycin oxidative damage to DNA. Talanta 56:959?970. https://doi.org/10.1016/S0039-9140(01)00656-7

54. Erdem A, Karadeniz H, Caliskan A (2009) Single-walled carbon nanotubes modified graphite electrodes for electrochemical monitoring of nucleic acids and biomolecular interactions. An Int J Devoted to Fundam Pract Asp Electroanal 21:464?471. https://doi.org/10.1002/elan.200804422

55. Vacek J (2009) Ex situ voltammetry and chronopotentiometry of Doxorubicin at a pyrolytic Graphite Electrode: Redox and Catalytic Properties and Analytical Applications. Electroanal An Int J Devoted to Fundam Pract Asp Electroanal 21:2139?2144. https://doi.org/10.1002/elan.200904646

56. Hynek D, Krejcova L, Zitka O et al (2012) Electrochemical study of doxorubicin interaction with different sequences of double stranded oligonucleotides, part II. Int J Electrochem Sci 7:34?49

57. Wong ELS, Gooding JJ (2007) The Electrochemical monitoring of the perturbation of charge transfer through DNA by Cisplatin. J Am Chem Soc 129:8950?8951

58. Hmoud Alotaibi S, Abdalla Momen A (2019) Anticancer drugs? deoxyribonucleic acid (DNA) interactions. Biophys Chem - Adv Appl. https://doi.org/10.5772/intechopen.85794

59. Pwavodi PC, Ozyurt VH, Asir S, Ozsoz M (2021) Electrochemical sensor for determination of various phenolic compounds in wine samples using Fe3O4 nanoparticles modified carbon paste electrode. Micromachines 12(3):312

60. Eksin E, Karadeniz H, Erdem A (2015) Voltammetric and impidimetric detection of Anticancer Drug Mitomycin C and DNA Interaction by using Carbon Nanotubes Modified Electrodes. Curr Bionanotechnol 1:32?36. https://doi.org/10.2174/2213529401666150218194827

61. Zhang K YZ (2010) Electrochemical behavior of adriamycin at an electrode modified with silver nanoparticles and multi-walled carbon nanotubes, and its application. Microchim Acta 169:161?165

62. Soleymani J, Hasanzadeh M, shadjou N, Jafari MK, Gharamaleki JV, AJ (2016) A new kinetic-mechanistic approach to elucidate electrooxidation of doxorubicin hydrochloride in unprocessed human fluids using magnetic graphene based nanocomposite modified glassy carbon electrode. Mat Sci Eng C 61:638?650

63. Chaney EN RPB (1982) Electrochemical determination of adriamycin compounds in urine by preconcentration at carbon paste electrodes. Anal Chem 54:2556?2560

64. Baldwin RP, Packett D TMW (1981) Electrochemical behavior of adriamycin at carbon paste electrodes. Anal Chem 53:540?542

65. Evtugyn G, Porfireva A, Stepanova V HB (2015) Electrochemical Biosensors based on native DNA and Nanosized Mediator for the detection of Anthracycline Preparations. Electroanalysis 27:629?637

66. Hashemzadeh N, Hasanzadeh M, Shadjou N, Eivazi-Ziaei J, Khoubnasabjafari M AJ (2016) Graphene quantum dot modified glassy carbon electrode for the determination of doxorubicin hydrochloride in human plasma. J Pharm Anal 6:235?241

67. Hajian R, Tayebi Z, Shams N (2017) Fabrication of an electrochemical sensor for determination of doxorubicin in human plasma and its interaction with DNA. J Pharm Anal 7:27?33. https://doi.org/10.1016/j.jpha.2016.07.005

Authors and Affiliations

Pwadubashiyi Coston Pwavodi[1]

✉ Pwadubashiyi Coston Pwavodi
ppwavodi@ciu.edu.tr

[1] Faculty of Engineering, Department of Biomedical Engineering, Cyprus International University, via Mersin 10, Haspolat, Nicosia, Northern Cyprus, Turkey